

## Two Characteristic H-bonded O–H Stretching Bands for the Compounds Containing Ether Oxygen and Hydroxyl Oxygen

Keiichi Ohno,\* Hiroshi Takao, Takashi Masuda, and Yukiteru Katsumoto

Department of Chemistry, Graduate School of Science, Hiroshima University, Kagamiyama, Higashi-Hiroshima 739-8526

(Received October 29, 2004; CL-041283)

The two characteristic H-bonded OH stretching bands of  $\alpha$ -monoalkyl- $\omega$ -hydroxyorigo(oxyethylene)s, ( $C_nE_m$ ), have been observed at about 3460 and 3330  $\text{cm}^{-1}$  in the liquid state; the former is due to the localized OH...O hydrogen bonds and the latter, the OH...OH...O hydrogen bonds of chain structures. The two bands were applied to the investigation of the phase transition process from the liquid to the solid for  $C_{12}E_3$ .

Self-organization of amphiphilic molecules which is one of the fundamental processes in solution chemistry is of great importance in biotechnology. Suitable probes are desired for elucidating those processes. In this paper, we report that the H-bonded OH stretching bands are usable as key bands for monitoring the structural behavior of nonionic surfactants,  $\alpha$ -monoalkyl- $\omega$ -hydroxyorigo(oxyethylene)s (abbreviated as  $C_nE_m$ ) even in states of complicated aggregation such as the liquid state. In the infrared spectra of  $C_nE_m$ , the sharp free OH stretching band is observed at about 3640  $\text{cm}^{-1}$  in  $\text{CCl}_4$  in analogy with primary

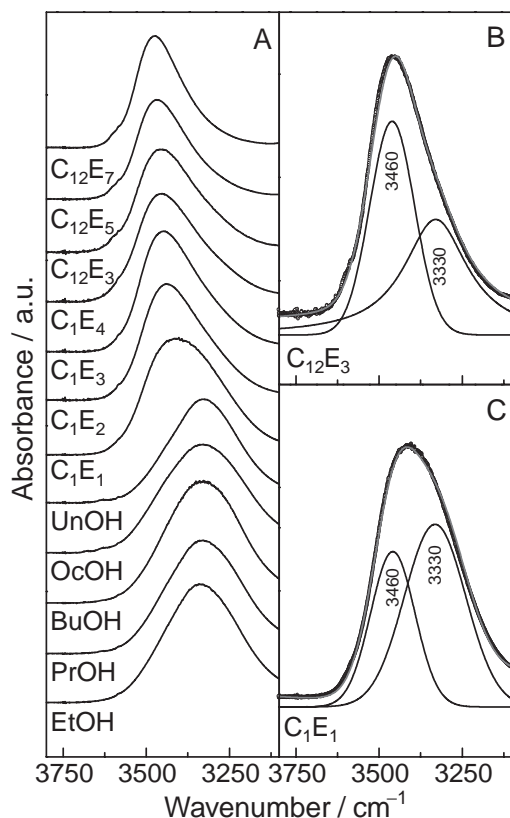


**Figure 1.** The H-bonded OH stretching bands of  $C_nE_m$  and primary alcohols in the liquid state.

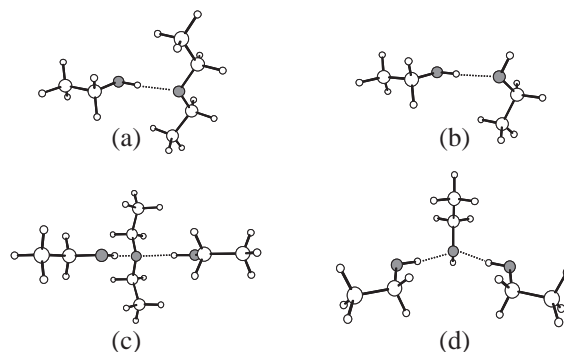


**Figure 2.** The localized OH...O hydrogen bonds optimized by the B3LYP/6-311++G(d,p).

alcohols.<sup>1</sup> The H-bonded OH stretching wavenumbers of 3460–3400  $\text{cm}^{-1}$  of  $C_nE_m$  in the liquid state, however, differ clearly from those of the alcohols, as given in Figure 1, indicating that the hydrogen bond of  $C_nE_m$  may be different from that of the alcohols in the liquid state. For all the alcohols, the H-bonded OH stretching bands are observed at about 3330  $\text{cm}^{-1}$  in the liquid state. It is well known that the free OH stretching band is shifted to lower wavenumbers upon the formation of hydrogen bonds and the magnitude of the red-shift is proportional to the strength of the hydrogen bond.<sup>2</sup> For  $C_nE_m$ , the band shape shows the overlapping of two major components. In fact, the broad bands can be resolved into two components, for example, the bands at 3460 and 3330  $\text{cm}^{-1}$  for  $C_{12}E_3$  and  $C_1E_1$  (B and C of Figure 1), by Gaussian–Lorentzian functions, though the broad band would be composed of many types of H-bonded OH vibrations. The relative intensity of the band at about 3460  $\text{cm}^{-1}$  increases with increasing the oxyethylene unit,  $m$ , of  $C_nE_m$ . This is interpreted that the population of the molecules concerned with the 3460  $\text{cm}^{-1}$  band increases compared to that concerned with the 3330  $\text{cm}^{-1}$  band. Recently, theoretical calculations such as B3LYP and MP2 methods give in general precise harmonic vibrational wavenumbers.<sup>3</sup> In order to confirm the above results, theoretical calculations by the B3LYP/6-311++G(d,p) method were performed for several H-bonded models.<sup>4</sup> In the calculations, diethyl ether ( $R_2O$ ) and ethyl alcohol ( $ROH$ ) were used as the simple model compounds for  $\text{CH}_2\text{CH}_2\text{OCH}_2\text{CH}_2-$  part and the  $-\text{CH}_2\text{CH}_2\text{OH}$  part of  $C_nE_m$ , respectively. The optimized geometries are shown in Figures 2 and 3. The harmonic OH stretching wavenumbers calculated are scaled by 0.93, because the calculated harmonic values are higher by about 10% than the observed unharmonic values.<sup>3</sup> The calculated H-bonded OH stretching wavenumbers are divided into two groups. One is 3412 (538)  $\text{cm}^{-1}$  for  $R_2O\cdots HOR$  (Figure 2a), 3424 (443)  $\text{cm}^{-1}$  for  $R(H)O\cdots HOR$  (Figure 2b), 3457 (371) and 3431 (511)  $\text{cm}^{-1}$  for  $ROH\cdots(R_2)O\cdots HOR$  (Figure 2c), and 3459 (360) and 3442 (511)  $\text{cm}^{-1}$  for  $ROH\cdots(RH)O\cdots HOR$

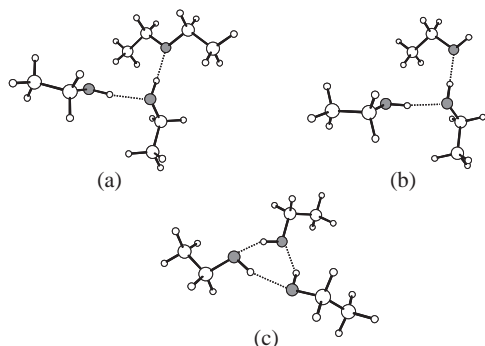


**Figure 3.** The OH...OH...O hydrogen bonds optimized by the B3LYP/6-311++G(d,p).

(Figure 2d), where the intensity,  $\text{km mol}^{-1}$ , is indicated in parentheses. Another is  $3355$  (626) and  $3320$  (787)  $\text{cm}^{-1}$  for  $\text{R}_2\text{O} \cdots \text{HO(R)} \cdots \text{HOR}$  (Figure 3a),  $3360$  (737) and  $3323$  (684)  $\text{cm}^{-1}$  for  $\text{R(H)O} \cdots \text{HO(R)} \cdots \text{HOR}$  (Figure 3b), and  $3360$  (754),  $3348$  (957), and  $3301$  (58)  $\text{cm}^{-1}$  for the cyclic trimer of ROH (Figure 3c). Thus, the calculated results indicate that the  $3460 \text{ cm}^{-1}$  band is associated with the localized OH...O hydrogen bond or the OH...O...HO hydrogen bond (the localized OH...O hydrogen bonds), as is likely to occur mainly for the hydrogen bond between OH and ether oxygen of  $\text{C}_n\text{E}_m$ . This band is experimentally found at about  $3470 \text{ cm}^{-1}$  for the cyclic dimer of  $\text{C}_1\text{E}_m$  ( $n = 1$  and  $2$ )<sup>5</sup> and at about  $3480 \text{ cm}^{-1}$  for the 8-membered-ring monomer of  $\text{C}_1\text{E}_m$  ( $n = 2$  and  $3$ ) in  $\text{CCl}_4$ .<sup>6</sup> The  $3330 \text{ cm}^{-1}$  band is associated with the OH...OH...O hydrogen bonds, as is likely to occur for hydrogen-bonding networks among hydroxyl groups of alcohols and also  $\text{C}_n\text{E}_m$ . It is therefore interpreted that for  $\text{C}_n\text{E}_m$  two characteristic bands are present in the liquid state; the localized OH...O hydrogen band at about  $3460 \text{ cm}^{-1}$  and the OH...OH...O hydrogen band of chain structures at about  $3330 \text{ cm}^{-1}$ .

The two bands were applied to the investigation of the phase

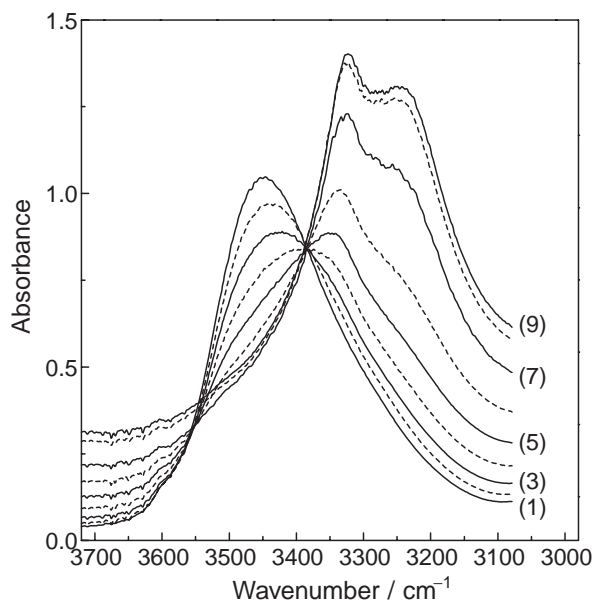


**Figure 4.** The spectral change in the phase transition from the liquid (1–4) to the solid (8, 9).

transition process from the liquid to the solid for  $\text{C}_{12}\text{E}_3$  at temperatures of 301 to 270 K. Figure 4 shows that the intensity of  $3460 \text{ cm}^{-1}$  band decreases, while that of the shoulder  $3330 \text{ cm}^{-1}$  band increases with decreasing temperature and then the  $3330 \text{ cm}^{-1}$  band is dominant and two new sharp bands appear, which are observed at  $3323$  and  $3250 \text{ cm}^{-1}$  at 270 K. The  $3323$ - and  $3250 \text{ cm}^{-1}$  bands should be assigned to the in-phase and out-of-phase modes, respectively, of the ordered  $(\cdots\text{OH} \cdots \text{OH} \cdots \text{OH})_n$  zigzag chain structures in the solid on the basis of the results of alcohols.<sup>7</sup> Thus, the above results indicate that the population of the hydrogen bond between OH and ether oxygen (the  $3460 \text{ cm}^{-1}$  band) decreases and that between OH and hydroxy oxygen with chain structures ( $3330 \text{ cm}^{-1}$ ) increases with decreasing temperature. The latter is predominant at the temperature immediately before solidification shown in 5 and 6 of Figure 4 (mp of  $\text{C}_{12}\text{E}_3$  is  $289.5$ – $290 \text{ K}$ <sup>8</sup>), and the latter with more strong intermolecular hydrogen bonds leads to the formation of the solid with the ordered  $(\cdots\text{OH} \cdots \text{OH} \cdots \text{OH})_n$  zigzag chain structures at the melting point or lower.

In conclusion, the two characteristic H-bonded OH stretching bands are present for  $\text{C}_n\text{E}_m$ ; the localized OH...O hydrogen band at about  $3460 \text{ cm}^{-1}$  and the OH...OH...O hydrogen band of chain structures at about  $3330 \text{ cm}^{-1}$ . The two key bands are useful for investigating the structural behavior of the compounds containing ether oxygen and hydroxyl oxygen such as  $\text{C}_n\text{E}_m$  in states of aggregation.

This work was partially supported by a Grant-in-Aid for Scientific Research on Priority Areas (417) from the Ministry of Education, Culture, Sports, Science and Technology (MEXT) of the Japanese Government.

## References

- 1 E. Nodland, *Appl. Spectrosc.*, **54**, 1339 (2000).
- 2 G. A. Jeffrey and W. Saenger, "Hydrogen Bonding in Biological Structures," Springer, Berlin (1994).
- 3 H. Yoshida, K. Takeda, J. Okamura, A. Ehara, and H. Matuura, *J. Phys. Chem. A*, **106**, 3580 (2002).
- 4 M. J. Frisch, G. W. Trucks, H. B. Schlegel, G. E. Scuseria, M. A. Robb, J. R. Cheeseman, V. G. Zakrzewski, J. A. Montgomery, Jr., R. E. Stratmann, J. C. Burant, S. Dapprich, J. M. Millam, A. D. Daniels, K. N. Kudin, M. C. Strain, O. Farkas, J. Tomasi, V. Barone, M. Cossi, R. Cammi, B. Mennucci, C. Pomelli, C. Adamo, S. Clifford, J. Ochterski, G. A. Petersson, P. Y. Ayala, Q. Cui, K. Morokuma, D. K. Malick, A. D. Rabuck, K. Raghavachari, J. B. Foresman, J. Cioslowski, J. V. Ortiz, B. B. Stefanov, G. Liu, A. Liashenko, P. Piskorz, I. Komaromi, R. Gomperts, R. L. Martin, D. J. Fox, T. Keith, M. A. Al-Laham, C. Y. Peng, A. Nanayakkara, C. Gonzalez, M. Challacombe, P. M. W. Gill, B. Johnson, W. Chen, M. W. Wong, J. L. Andres, C. Gonzalez, M. Head-Gordon, E. S. Replogle, and J. A. Pople, "Gaussian 98, Revision A.5," Gaussian, Inc., Pittsburgh, PA (1998).
- 5 T. Masuda, H. Takao, Y. Katsumoto, H. Sugeta, and K. Ohno, unpublished data.
- 6 F. A. J. Singelenberg, E. T. G. Lutz, J. H. van der Maas, and G. Jalsovszky, *J. Mol. Struct.*, **235**, 173 (1991).
- 7 D. Schioberg, T. Mentel, and W. A. P. Luck, *J. Mol. Struct.*, **129**, 237 (1985) and references cited therein.
- 8 Y. Abe and S. Watanabe, *Kagaku Kogaku*, **66**, 86 (1963).